Cellular Microbiology (2011) doi:10.1111/j.1462-5822.2011.01611.x

Pseudomonas aeruginosa interacts with epithelial cells rapidly forming aggregates that are internalized by a Lyn-dependent mechanism

Paola Lepanto,[1] David M. Bryant,[2,3] Jéssica Rossello,[1] Anirban Datta,[2,3] Keith E. Mostov[2,3] and Arlinet Kierbel[1]*

[1]*Institut Pasteur de Montevideo, Montevideo 11400, Uruguay.*

Departments of [2]Anatomy and [3]Biochemistry and Biophysics, University of California, San Francisco, CA 94143, USA.

Summary

Growing evidence is pointing to the importance of multicellular bacterial structures in the interaction of pathogenic bacteria with their host. Transition from planktonic to host cell-associated multicellular structures is an essential infection step that has not been described for the opportunistic human pathogen *Pseudomonas aeruginosa*. In this study we show that *P. aeruginosa* interacts with the surface of epithelial cells mainly forming aggregates. Dynamics of aggregate formation typically follow a sigmoidal curve. First, a single bacterium attaches at cell–cell junctions. This is followed by rapid recruitment of free-swimming bacteria and association of bacterial cells resulting in the formation of an aggregate on the order of minutes. Aggregates are associated with phosphatidylinositol 3,4,5-trisphosphate (PIP3)-enriched host cell membrane protrusions. We further show that aggregates can be rapidly internalized into epithelial cells. Lyn, a member of the Src family tyrosine kinases previously implicated in *P. aeruginosa* infection, mediates both PIP3-enriched protrusion formation and aggregate internalization. Our results establish the first framework of principles that define *P. aeruginosa* transition to multicellular structures during interaction with host cells.

Received 14 January, 2011; revised 8 April, 2011; accepted 11 April, 2011. *For correspondence. E-mail arlinet.kierbel@pasteur.edu.uy; Tel. (+598) 2 522 0910; Fax (+598) 2 522 4185.

Introduction

Pseudomonas aeruginosa is a ubiquitous environmental bacterium that is capable of causing acute infections in individuals with wounds or those with immune defects, as well as chronic infections with high mortality in cystic fibrosis (CF) patients. Current concepts propose that biofilm formation is a key factor in *P. aeruginosa* CF-associated airway infections (Moreau-Marquis *et al.*, 2008a; Hall-Stoodley and Stoodley, 2009). Bacterial biofilms are communities of cell aggregates attached to living or abiotic surfaces embedded in an extracellular matrix (Costerton *et al.*, 1999). Interaction with host cells forming multicellular structures is thought to be a common feature among pathogenic bacteria, and is frequently observed *in vivo* (Clausen and Christie, 1982; Menozzi *et al.*, 1994; Hassett *et al.*, 2010). Many pathogenic bacteria attach to the surface of cells forming microcolonies or aggregates. Several lines of evidence support the notion that aggregation is an important virulence mechanism. For example, aggregated *S. pyogenes* bacteria adhere more efficiently to epithelial cells than do non-aggregating *S. pyrogenes*, and unlike the latter, survive and grow in the human bloodstream (Frick *et al.*, 2000). Type IV pili-mediated cell aggregation is a prerequisite for *N. gonorrhoeae* adhesion to host cells (Park *et al.*, 2001). Finally, transition from a planktonic state to surface-associated clusters is required for biofilm formation (Stoodley *et al.*, 2002; Lemon *et al.*, 2008). Although attaching in clusters seems to be a common feature for pathogenic bacteria, there are many different ways cluster formation is achieved. For example, individual *N. meningitidis* cells attach to the surface of endothelial cells and then proliferate to form large aggregates or microcolonies (Mairey *et al.*, 2006). Large aggregates of *Bartonella henselae* are formed on the surface of endothelial cells after cellular contact is established with a leading lamella and bacteria. Subsequently, bacterial aggregation is mediated by rearward transport on the cell surface (Dehio *et al.*, 1997). The process by which *P. aeruginosa* makes the transition from planktonic to host-associated aggregates, however, has not been described to date.

After associating with the host cell surface, *P. aeruginosa* can become intracellular. About 50% of clinical

isolates studied can be measurably internalized into non-phagocytic cells both *in vivo* and *in vitro* (Engel, 2003). The role of internalization in the infection process, however, is not clearly understood. Cellular uptake of *P. aeruginosa* might permit intracellular replication in a host environment in which it is protected from the immune system. Uptake might facilitate transcytosis across epithelial cells, allowing access to deeper tissues. Alternatively, it might be beneficial for the host, as a defence mechanism (Pier *et al*., 1996; Pier *et al*., 1997). Likewise, the involvement of host signal transduction pathways in *P. aeruginosa* internalization is poorly understood. Entry relies on the actin cytoskeleton and is accompanied by activation of Rho family GTPases, known regulators of the actin cytoskeleton (Evans *et al*., 1998; Kazmierczak *et al*., 2001; Darling *et al*., 2004; Pielage *et al*., 2008). Infection results in tyrosine phosphorylation of several host proteins including members of Src family tyrosine kinases (SFKs) Src, Fyn and Lyn (Evans *et al*., 1998; Esen *et al*., 2001; Kannan *et al*., 2006; Kannan *et al*., 2008). A role for SFKs member Lyn in *P. aeruginosa* internalization has been reported (Kannan *et al*., 2006; Kannan *et al*., 2008). We previously demonstrated that activation of phosphatidylinositol 3-kinase (PI3K) and Akt is necessary for *P. aeruginosa* entry from the apical surface of polarized epithelial cells (Kierbel *et al*., 2005). We further showed that large membrane protrusions enriched for *de novo* synthesized phosphatidylinositol 3,4,5-trisphosphate (PIP3) and actin formed at the apical surface at the site of bacterial attachment (Kierbel *et al*., 2007). In those studies we observed *P. aeruginosa* often attached to the apical surface as bacterial aggregates.

In the present work we investigate the origin of those aggregates and their implication in the host cell response elicited by *P. aeruginosa* infection.

We found that *P. aeruginosa* makes the transition from planktonic to host cell-attached aggregates on the order of minutes by recruitment of free-swimming bacteria to localized spots on the cell surface. Aggregates are associated with the previously described host-membrane protrusions and can be internalized into epithelial cells. We found that SFKs member Lyn mediates both PIP3-enriched protrusion formation and aggregate internalization.

Results

P. aeruginosa *attaches mainly as aggregates to the apical surface of epithelial cells*

We have previously observed the presence of bacterial aggregates on the surface of cultured epithelial cells after infection with *P. aeruginosa* strain K (Kierbel *et al*., 2007). To analyse and quantify cell-associated aggregation, Madin–Darby canine kidney (MDCK) cells expressing the pleckstrin homology (PH) domain of Akt fused to GFP (PH-Akt-GFP) were infected with *P. aeruginosa* harbouring fluorescent monomeric protein 'Cherry' (m-Cherry). The PH domain of Akt is a protein probe for PIP3 that normally localizes to the basolateral surface in polarized MDCK cells (Yu *et al*., 2005). Infections were carried out for 30 min using *P. aeruginosa* grown to stationary phase. Samples were then fixed and visualized either by scanning electron or laser confocal microscopy. Figure 1A shows scanning electron microscopy images of aggregates adhered to the apical surface of MDCK cells. Individually attached bacteria and bacterial aggregates were counted in z-stack images of ~ 10 randomly chosen fields in four independent experiments (Fig. 1B). An aggregate was defined as a cluster of 6 or more bacteria. The average number of individually attached bacteria per field was 18 ± 3 (82% of total association events), while the average number of aggregates per field was 4 ± 0.2 (18% of total association events) (Fig. 1C). The total number of bacteria contained in aggregates was estimated as described in *Experimental procedures*. It should be noted that the number of bacteria per aggregate was highly variable, ranging from 6 to ~ 300. We found that 94 ± 1% of cell-surface associated bacteria formed part of the aggregates (Fig. 1C). Thus, *P. aeruginosa* attachment to epithelial cells mostly involved forming multicellular structures. Remarkably, aggregates but not individual bacteria were found primarily at cell–cell junctions (Fig. 1D).

P. aeruginosa *aggregates are formed rapidly on cell surface by recruitment of free-swimming bacteria*

Aggregation of *P. aeruginosa* cells in liquid culture has been reported previously (Allesen-Holm *et al*., 2006; Schleheck *et al*., 2009). We wondered whether cell-associated aggregates found 30 min after inoculation had formed previously in liquid culture or only after individual bacteria contacted epithelial cells. To distinguish between these two possibilities two *P. aeruginosa* cultures, one expressing GFP and one expressing m-Cherry, were grown to stationary phase. Cultures were then mixed in equivalent amounts and used to infect MDCK cells at a multiplicity of infection (moi) of 60 for 30 min. If aggregates had formed previously in the liquid medium, they should have a single colour, whereas if they formed on the cell surface they should have two colours. All aggregates analysed in three independent experiments had two colours, indicating that, at least to some extent, aggregation took place on the cell surface (Fig. 2A and B). We next monitored the aggregate formation process by live z scanning video microscopy (Video S1 and Fig. 2C). Aggregates were formed *de novo* on cell surface by free-swimming bacteria recruited to localized spots. To

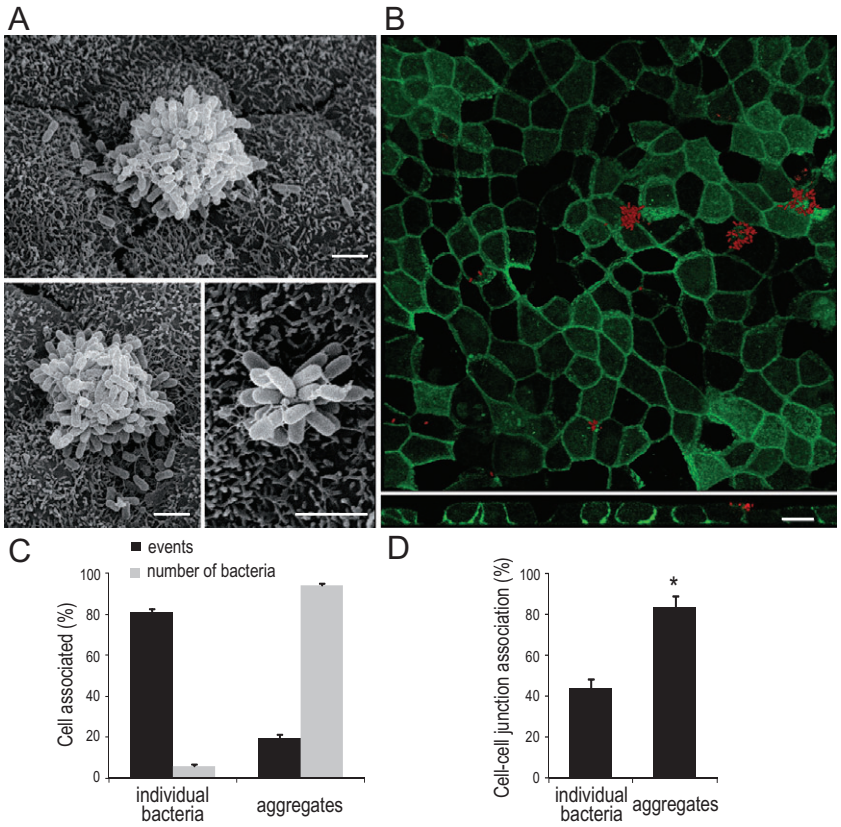

Fig. 1. *P. aeruginosa* attaches to the surface of epithelial cells mainly as aggregates. MDCK cells were grown on filters as polarized monolayers and infected with stationary phase-grown *P. aeruginosa* for 30 min.
A. Scanning electron micrographs of *P. aeruginosa* aggregates attached to the apical surface of MDCK cells. Scale bar: 2 μm.
B. 3D reconstruction of a representative confocal image stack of MDCK cells stably expressing GFP-PH-Akt (green) infected with m-Cherry *P. aeruginosa* (red). Bacterial aggregates as well as individual bacteria are seen adhered to the cell surface. An orthogonal section is shown below. Scale bar: 20 μm.
C. Black bars: percentage of cell-associated events represented by individually attached bacteria or by aggregates. Grey bars: number of bacteria associated to cells individually or in aggregates (percentage of the total).
D. Percentage of individually attached bacteria or aggregates bound to cell–cell junctions. Data are represented as mean ± standard deviation, *$P < 0.05$.

analyse the dynamics of bacterial cell attachment, integrated fluorescence intensity was plotted over time (Fig. 2D). Adhesion kinetics displayed three distinct phases. The initial phase was characterized by the binding of a single bacterium, which we designated as the founder that remains attached alone for several minutes. Occasionally, a second bacterium was seen to attach near the founder prior to growth of the aggregate. After binding of the second or third bacterium, the adhesion kinetics profile changed to a sudden increase to result in the formation of the aggregate. This exponential growth phase typically lasted between 2 and 4 min. Finally aggregate growth reached a plateau. Consistently with SEM and fluorescence microscopy snapshots, founding bacteria attached to cell–cell junctions, suggesting that a specific host cell factor present at that location stimulates bacterial aggregation. To our knowledge this is the first report of the dynamics of *P. aeruginosa* host cell surface colonization.

P. aeruginosa *aggregates are associated with host cell membrane protrusions and can be internalized into epithelial cells*

We have previously shown that attachment of *P. aeruginosa* to the apical surface of MDCK cells is associated with the formation of large host cell membrane protrusions. These protrusions are enriched in PIP3, a lipid that usually localizes to the basolateral surface of uninfected polarized MDCK but accumulates apically upon bacterial binding (Kierbel *et al.*, 2007). We wanted to determine if protrusion formation was associated with bacterial aggregates, individual bacteria, or both. PH-Akt-GFP MDCK cells were infected with m-Cherry *P. aeruginosa* for 30 min, fixed and examined by confocal microscopy. The number of single bacterium-associated protrusions or bacterial aggregate-associated protrusions was determined for ~7 fields in 4 independent experiments. Protrusion formation was acknowledged as such when apical accumulation of PIP3 was found (Fig. 3A, left panel). Protrusion formation was clearly associated with bacterial aggregates (Fig. 3B). However, it cannot be ruled out that PIP3 also associates with individual bacteria at a level below the detection threshold with the PH-Akt probe. Our previous studies suggested that these membrane protrusions are transient structures formed at a stage in the bacterial internalization process. Thus, protrusion formation as well as *P. aeruginosa* internalization depended on both actin polymerization and PI3K activity (Kierbel *et al.*, 2005; Kierbel *et al.*, 2007). Since the protrusions were associated with aggregates, we wanted to determine if these multicellu-

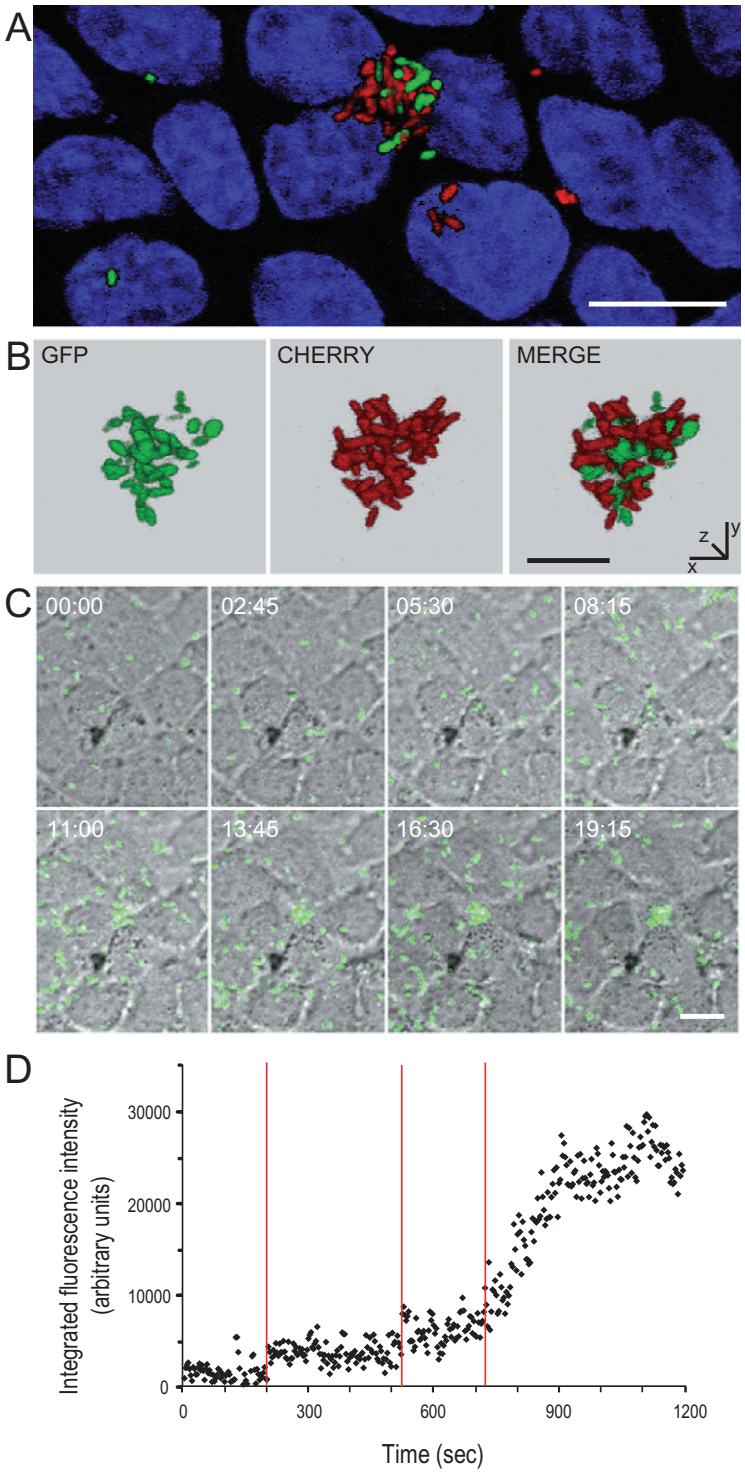

Fig. 2. *P. aeruginosa* aggregates are formed on the apical cell surface.
A and B. 3D reconstructions of confocal image stacks of filter grown MDCK cells infected for 30 min with a 1:1 mix of GFP *P. aeruginosa* and m-Cherry *P. aeruginosa*. Cultures were grown separately to stationary phase and mixed immediately prior to infection. (A) Nuclei were stained with TOPRO. Scale bar: 10 μm. (B) Scale bar: 5 μm.
C. Montage from a representative time-lapse microscopy video. Polarized MDCK grown on glass bottom dishes were infected with GFP *P. aeruginosa*. Images were collected every 3 s beginning immediately after bacterial inoculation. Aggregates were formed from free-swimming bacteria that were recruited to cell–cell junctions. Scale bar: 10 μm, time is indicated in min : s.
D. Dynamics of bacterial attachment. Integrated fluorescent intensity at the site of aggregate formation is plotted over time. Vertical lines indicate the time at which a first, second and third bacterium attached.

lar bacterial structures could internalize into epithelial cells. Confocal images of cells infected for 2 h exhibited extracellular as well as partially and completely internalized aggregates (Fig. 3A). Three independent experiments were done to quantify the internalization of individual bacteria and aggregates. Figure 3C shows the number of intracellular individual bacteria and aggregates after 2 h infection as a function of cell-associated individual bacteria or aggregates respectively. Internalization was comparable between both groups. We then estimated the number of bacteria forming part of internalized aggregates. This value represented 59 ± 12% of

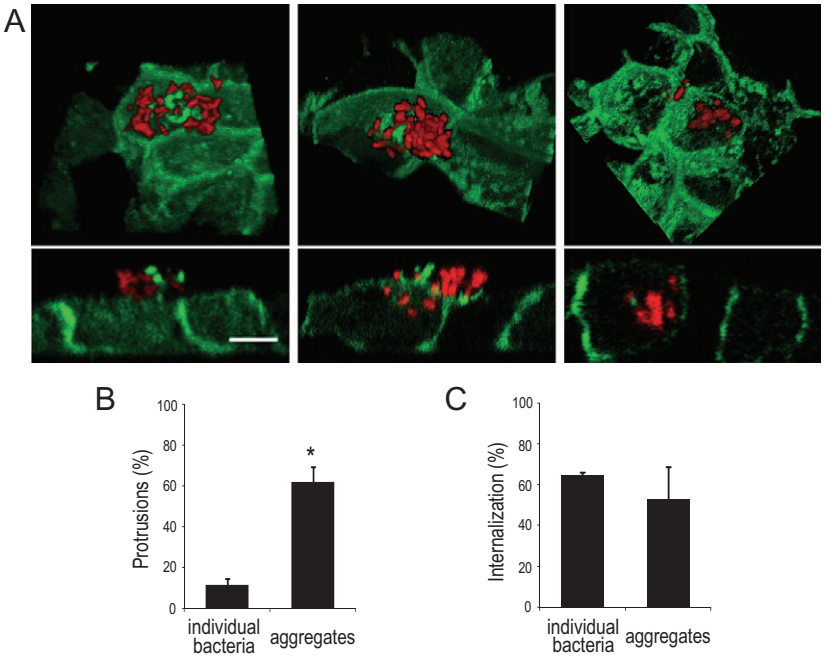

Fig. 3. Aggregates are associated with PIP3-enriched protrusions and can be internalized into epithelial cells.
A. 3D reconstructions (upper images) and orthogonal sections (lower images) from stacks of images of GFP-PH-Akt MDCK cells infected with m-Cherry *P. aeruginosa*. Images show representative sequential stages in the process of aggregate internalization. From left to right: extracellular aggregate associated with a PIP3-enriched protrusion, partially internalized aggregate, intracellular aggregate. Scale bar: 5 μm.
B. Percentage of individually attached bacteria or aggregates associated with PIP3-enriched protrusions.
C. Percentage of internalized individual bacteria or aggregates relative to cell associated individual bacteria or cell associated aggregates respectively. Data are represented as mean ± standard deviation, *$P < 0.05$.

total internalized bacteria. This value was smaller than the estimated number of bacteria forming part of the aggregates on the cell surface (94%). This is consistent with the inability of larger aggregates to internalize during the time-course of our experiment. In conclusion, aggregates are preferentially associated to PIP3-enriched protrusions and can be internalized into epithelial cells.

Formation of aggregate-associated protrusions is dependent on Src family tyrosine kinases

SFKs members are related non-receptor tyrosine kinases that participate in various processes, such as control of cell adhesion or cell migration. They are known to regulate cytoskeletal changes leading to the formation of the phagocytic cup and eventual internalization of particles (Suzuki *et al*., 1998; Furumoto *et al*., 2004) as well as to stimulate Rac-mediated formation of membrane protrusions at the leading edge of migrating cells (Guarino, 2010). We previously reported that the PI3K/Akt pathway is activated upon infection of MDCK cells with *P. aeruginosa* grown to stationary phase, and that activation of this pathway is important for *P. aeruginosa* internalization (Kierbel *et al*., 2005). Requirement of this pathway for *P. aeruginosa* entry into phagocytic cells was later also demonstrated (Kannan *et al*., 2008; Chung *et al*., 2009). Class IA PI3Ks can be activated by receptor or non-receptor tyrosine kinases (Hawkins *et al*., 2006). PI3K activation leads to the production of PIP3, which recruits protein kinase Akt to the membrane through its PH domain (Susa *et al*., 1996; Vanhaesebroeck and Alessi, 2000). Once in the membrane Akt is phosphorylated leading to activation of its kinase activity. Here, we tested whether SFKs are required for activation of PI3K/Akt by *P. aeruginosa* in MDCK epithelial cells. To do this, the effect of SFKs inhibitor SU6656 on the levels of phosphorylated (i.e. activated) Akt was assessed. Treatment with 10 μM SU6656 slightly reduced the amount of phosphorylated Akt; however, the change was not statistically significant (Fig. 4A and B). SFKs activation was measured using an anti Src-Family phospho-Tyr 416 antibody. This antibody detects endogenous levels of Src and other Src family members only when phosphorylated at tyrosine 416 or equivalent activation sites. The active conformation of SFKs becomes stabilized upon autophosphorylation of Tyr 416 (Engen *et al*., 2008). As shown in Fig. 4A (lower panel), the level of activated SFKs was increased in *P. aeruginosa* infected cells whereas the level of housekeeping protein GAPDH was unaffected. Activation was strongly inhibited by SU6656. The total level of the members of this protein family that is produced in MDCK cells (Src, Lyn, Fyn, Yes and Lck) remained unchanged (data not shown). We then tested whether SFKs were involved in formation of PIP3-enriched membrane protrusions. To assess this PH-AKT-GFP MDCK cells were infected with m-Cherry *P. aeruginosa* for 30 min in the presence or absence of 10 μM SFKs inhibitor PP2. SU6656 was not used in these experiments since it exhibits autofluorescence. As noted above, apical accumulation of PIP3 was correlated with protrusion formation. Following this criterion, surface-attached aggregates were classified as associated or non-associated with cell membrane protrusions. As shown in Fig. 4C and D, treatment with PP2 reduced the

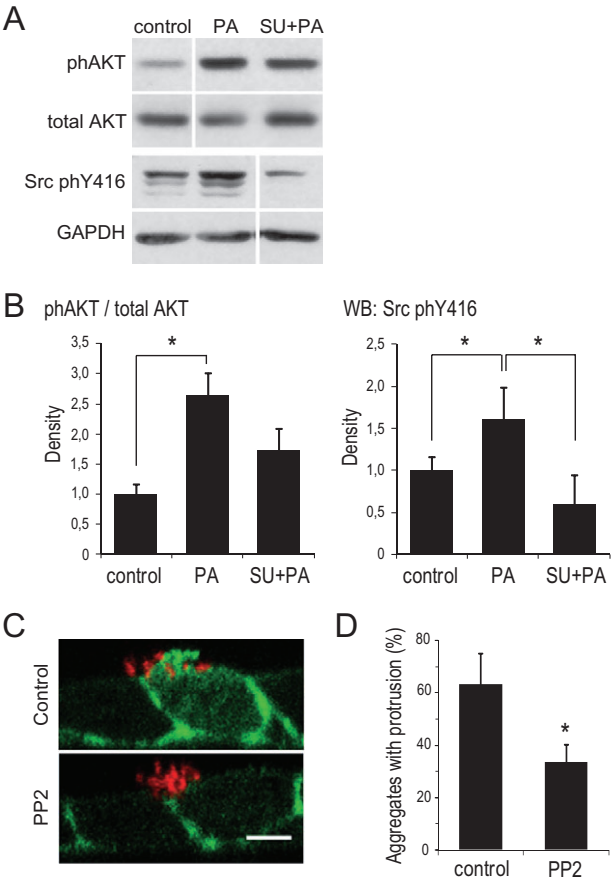

Fig. 4. PIP3-enriched protrusion formation is mediated by Src family tyrosine kinases.
A. MDCK cells were infected with *P. aeruginosa* for 1 h. Cell lysates were examined by immunoblot with the antibodies indicated. SFKs inhibitor SU6656 (10 μm) does not significantly modify *P. aeruginosa*-dependent PI3K/Akt activation while completely blocked activation of SFKs. Samples run in non-adjacent lanes of the same gel are shown separately.
B. Quantification of PI3K/Akt and SFKs activation.
C. Orthogonal sections from representative confocal images stacks of GFP-PH-Akt MDCK cells infected with m-Cherry *P. aeruginosa* for 30 min. Treatment with SFKs inhibitor PP2 (10 μm) reduced the number of aggregate-associated protrusions. Scale bar: 5 μm.
D. Quantitative analysis of PP2 treatment on formation of aggregate associated protrusions. Data are represented as mean ± standard deviation, *P < 0.05.

number of *P. aeruginosa* aggregate-associated protrusions. Thus, SFKs are activated after MDCK cells are inoculated with *P. aeruginosa* and activation is important for formation of PIP3-enriched protrusion.

Entry of P. aeruginosa *aggregates is dependent on Src family tyrosine kinases*

Previous studies provided evidence for a role for SFKs in the internalization of *P. aeruginosa* in different cell lines (Evans *et al.*, 1998; Esen *et al.*, 2001). We performed standard invasion assays while inhibiting SFKs to test for the involvement of this regulatory pathway in our system. Both PP2 (10 μM) and SU6566 (10 μM) decreased internalization of *P. aeruginosa* into MDCK cells without affecting adhesion (Fig. S1). Standard invasion assays do not distinguish between entry of individual and aggregated bacteria, and our results showing that SFKs plays a role in protrusion formation suggested that this family might be important for aggregate internalization. To evaluate this, bacterial internalization was analysed by confocal microscopy. As compared with untreated controls, treatment with SFKs inhibitor PP2 decreased both the number of internalized individual bacteria as well as the number of internalized aggregates (Fig. 5A and B), suggesting they use the same internalization pathway. Consistently, inhibition of PI3K abrogates both, individual and aggregated bacterial entry (data not shown). SFKs inhibitor SU6656 produced similar results than PP2 (data not shown).

SFKs member Lyn is important for both protrusion formation and aggregate internalization

SFKs member Lyn has been previously linked to *P. aeruginosa* internalization (Kannan *et al.*, 2006; Kannan *et al.*, 2008). To determine if this was the SFKs member responsible for the observed phenotypes, MDCK cells with reduced expression of Lyn were used in standard invasion and adhesion assays. Knock-downs were generated using short hairpin RNA (shRNA). Two different shRNAs were tested. Cells with reduced expression of Lyn showed a decrease in *P. aeruginosa* internalization compared with cells expressing scramble shRNA, and in which adhesion was unaffected (Fig. S2). We next evaluated the effect of reduced Lyn expression on *P. aeruginosa*-PI3K/Akt activation, protrusion formation and individual bacteria and aggregate internalization. Levels of Akt phosphorylation were compared between scramble and Lyn shRNA expressing cells. Reduced expression of Lyn resulted in significant inhibition of *P. aeruginosa*

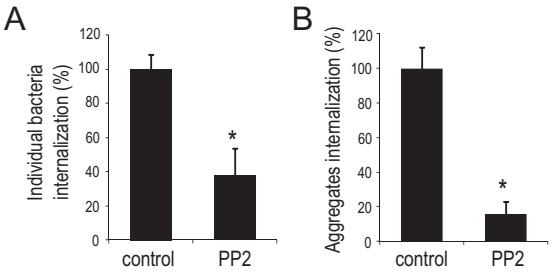

Fig. 5. Entry of *P. aeruginosa* aggregates is dependent on Src family tyrosine kinases. GFP-PH-Akt MDCK cells were infected with m-Cherry *P. aeruginosa* for 2 h. Treatment with SFKs inhibitor PP2 (10 μm) reduced the percentage of internalized individual bacteria (A) and aggregates (B). Data are represented as mean ± standard deviation, *P < 0.05.

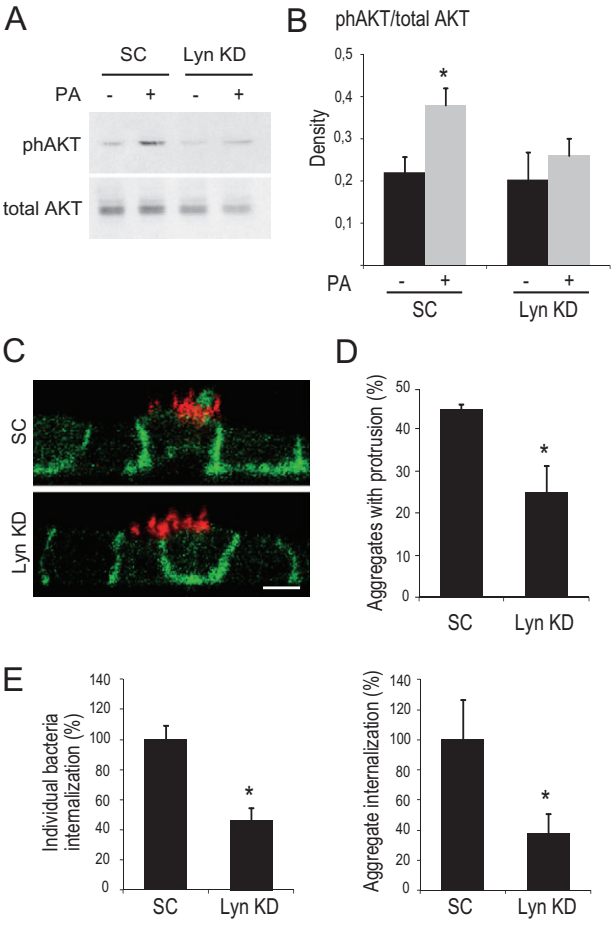

Fig. 6. Decreased expression of Lyn reduces protrusion formation and aggregate internalization.
A and B. MDCK cells expressing scramble or Lyn shRNA were infected with *P. aeruginosa* for 1 h. Cell lysates were examined by immunoblot with the antibodies indicated. Decreased expression of Lyn reduced *P. aeruginosa* dependent PI3K/Akt activation (quantitatively measured in B).
C and D. Orthogonal sections from representative confocal images stacks of GFP-PH-Akt MDCK cells expressing scramble or Lyn shRNA and infected with m-Cherry *P. aeruginosa* for 30 min. Reduction of Lyn expression reduced the number of aggregate-associated protrusions (quantitatively measure in D) Scale bar: 5 μm.
E. Reduced expression of Lyn decreased individual bacteria as well as aggregate internalization. SC: scramble, KD: knock-down. Data are represented as mean ± standard deviation, *$P < 0.05$.

dependent PI3K/Akt activation (Fig. 6A and B). Akt-PH-GFP MDCK cells expressing scramble or Lyn shRNA were infected with m-Cherry *P. aeruginosa* for 30 min or 2 h. Protrusion formation (30 min infections) and bacterial internalization (2 h infections) were evaluated as described above. Reduced expression of Lyn inhibited both protrusion formation (Fig. 6C and D) as well as individual bacterial and aggregate internalization (Fig. 6E, left and right panel respectively). Thus, reduced expression of Lyn resulted in the same effect on protrusion formation and internalization found with pharmacological inhibition of SFKs, leading to the conclusion that Lyn is the member of the Src family involved in these processes.

Discussion

We here show that *P. aeruginosa* interacts with the surface of epithelial cells, forming multicellular structures. A large portion of newly formed aggregates is internalized into epithelial cells within 2 h of inoculation. We observed that groups containing from 6 to up to ~ 30 bacteria enter the cell during aggregate internalization. Entry as a group might increase the chances of intracellular survival. The concentration of bacterial factors necessary for intracellular establishment or the efficient exit from the cell would be enhanced with increased numbers of bacteria. Alternatively, if the aggregate dissociated inside the cell, multiple intracellular destinations could be reached rapidly and, overall, bacteria would have more chances to find a niche appropriate for replication. On the contrary, collective internalization could be part of a mechanism by which epithelial cells dispose of bacterial cells.

Through shRNA loss of function experiments we found that Lyn is required for the internalization of *P. aerugionsa* into MDCK cells. Lyn was previously linked to *P. aeruginosa* internalization, both in alveolar epithelial cells and in macrophages (Kannan *et al*., 2006; Kannan *et al*., 2008). Lyn was also reported to bind to and activate PI3K and Akt to regulate phagocytosis of *P. aeruginosa* in alveolar macrophages by a membrane raft-dependent pathway. In agreement with this, we found that Lyn acts upstream of *P. aeruginosa* dependent Akt/PI3K activation in epithelial cells. However, in our system, biochemical inhibition of SFKs did not significantly reduce Akt/PI3K activation by *P. aeruginosa*. A possible explanation could be an antagonistic effect of other SFKs member/s in *P. aeruginosa*-dependent PI3K activation in epithelial cells. In this report we demonstrate that SFKs and, in particular Lyn, are important for aggregate-associated protrusion formation. Furthermore, we also show that Lyn is crucial for aggregate internalization. These results support our previously reported idea that formation of PIP3-enriched protrusions is part of a mechanism of *P. aeruginosa* internalization. As noted above, activation of PI3K by SFKs has been reported in several systems. Lyn was also shown to interact directly with the p85 subunit of PI3K using a yeast two-hybrid assay (Zhu *et al*., 2006). Thus, our model postulates that formation of *P. aeruginosa* aggregates on the surface of epithelial cells results in activation of Lyn tyrosine kinase that in turn leads to PI3K activation and subsequent PIP3 apical accumulation. Apical PIP3 accumulation then leads to protrusion formation and aggregate internalization. Kannan *et al*. (2006) postulated that activation of Lyn by *Pseudomonas* resulted in apoptosis of epithelial alveolar cells after 2 h infection. Although we

cannot rule out induction of apoptosis in our system, cell viability remained above 99% up to 9 h after inoculation (data not shown).

Association of bacteria with host cells as multicellular aggregates is emerging as a common feature in pathogenic bacteria-host interactions. Surface attachment and microcolony formation are early key steps in biofilm development. The presence of biofilms is linked to the acquisition of both antibiotic and host immune system resistance in *P. aeruginosa* infections. Importantly, recent studies suggested that biofilms that form on abiotic surfaces are different in several important ways from biofilms that form on epithelial cells (Moreau-Marquis *et al.*, 2008a,b). Thus, a detailed understanding of the transition from planktonic to cell-associated multicellular structures could be essential for developing strategies to control a range of bacterial infections. In this study we described *P. aeruginosa* surface aggregation dynamics into distinct phases. In an initial lag phase a single bacterial cell attaches and remains alone (occasionally a second bacterium attaches nearby). This is followed by a rapid increase of binding characterized by bacterial cell–cell association that results in aggregate formation. Does something that takes place during the lag phase trigger subsequent collective attachment? Binding of the founder bacterium to the host membrane might induce localized release of a substance(s) from the host cell that attracts free-swimming bacteria. Dacheux *et al.* (2001), for example, described the pack swarming phenomenon in cytotoxic strains of *Pseudomonas aeruginosa*. In that study, highly motile bacteria were observed to surround wounded macrophage cells in response to chemotactic signal molecules released from the macrophage. The authors postulated that these molecules were released through small pores in macrophage membranes previously generated by the Pseudomonas type III secretion system. Alternatively, the founder might release a chemoattractant upon attachment to epithelial cells. It has been shown that under certain stress conditions *Escherichia coli* and *Salmonella typhimurium* excrete chemotactic molecules that attract other bacteria leading to the formation of dense multicellular clusters (Budrene and Berg, 1991; 1995).

In summary, our studies showed that *P. aeruginosa* undergoes a transition from planktonic to cell surface attached mainly by forming aggregates. Some bacterial clusters become intracellular soon, while others, including those of larger size, remain surface attached. Future studies will elucidate the signalling that mediates coordinated behaviour and formation of multicellular structures as well as address the fate of extra and intracellular aggregates. If internalization is a mechanism by which epithelial cells dispose of bacteria, rapid aggregation of bacteria into large aggregates may be a way to avoid internalization. Furthermore, those aggregates that remain extracellular could then evolve to form mature biofilms.

Finally, we believe that detailed understanding of the transition from planktonic to cell-associated multicellular structures could be of relevance to develop strategies to control such biofilm-related infections.

Experimental procedures

Antibodies and reagents

Antibodies against total Akt, Akt phosphorylated on serine 473, Src-Family phospho-Tyr 416 and Lyn were obtained from Cell Signaling Technology (Beverly, MA, USA). Anti-GAPDH mAb from Chemicon International (Temecula, CA, USA). SU6656 and PP2 were purchased to Sigma-Aldrich (St. Louis, MO, USA).

Cell preparation and culture

Wild-type MDCK (clone II) and MDCK stably transfected with GFP–PH–Akt (Yu *et al.*, 2005) were cultured in minimal essential medium (MEM) containing 5% fetal bovine serum at 37°C with 5% CO_2. Cells were seeded (1×10^6 cells per well) on six-well culture plates or trans-wells (0.4 μm pore size, Corning Fisher, NY, USA) and used for experiments after 24 h in culture.

For video microscopy studies wild-type MDCK cells were grown on glass bottom microwell dishes (MatTek Corporation, Ashland, MA, USA). Cells were seeded at a density of ~ 100 000 cells cm^{-2} and grown for 4 days to ensure the formation of fully polarized monolayers (Kreitzer *et al.*, 2003).

Bacterial infection

Pseudomonas aeruginosa strain K was routinely grown shaking overnight in Luria-Bertani broth at 37°C. For fluorescence microscopy studies *P. aeruginosa* carrying plasmids containing either m-Cherry (Mougous *et al.*, 2007) or GFP (Bucior *et al.*, 2010) genes were used. Stationary phase bacteria were co-cultivated with MDCK monolayers at the indicated moi. Standard adhesion and internalization assays were performed as described previously (Kazmierczak *et al.*, 2001). For inhibitor treatments, cells were pre-incubated for 1 h with MEM containing the drug at indicated concentrations. Bacterial inoculations were carried out in the presence of the drug.

Microscopy studies

Bacteria were incubated with filter grown MDCK monolayers (moi of 150, unless otherwise indicated) for indicated times and washed three times with phosphate-buffered saline (PBS). For fluorescent microscopy studies, samples were fixed with 4% paraformaldehyde for 30 min at room temperature and examined with a confocal microscope (Leica TCS-SP5) using a HCX PL APO 63/1.4–0.60 CS oil objective. For scanning electron microscopy samples were fixed with 2% cacodylate gluteraldehyde then treated using standard procedures and analysed with a Jeol (JSM-5900LX) microscope.

Live-cell time-lapse video microscopy

Wild-type MDCK cells were grown on glass bottom microwell dishes as described above. Microwell dishes were placed on microscope stage and cells were infected with GFP–*P. aeruginosa* (moi of 60). An enclosed stage allowed for temperature and CO_2 enrichment control. A z-stack of images (7 planes at 1 μm spacing) was collected every 3 s for 30 or 40 min in randomly chosen fields.

Image analysis

Images were analysed using the Image J program (National Institutes of Health, NIH). The confocal image stacks were projected along the z-axis, creating an output image in which each pixel contained the sum over z of the pixel intensity values in that particular x–y position. Finally, Integrated fluorescence intensity was quantified in the region of interest.

The number of bacteria in an aggregate was obtained from the ratio between aggregate volume and volume of one bacterium. Volumes were estimated using the Object Counter 3D plug-in. For each field analysed, a specific single bacterium average volume was established.

Cell lysates and Western blot

MDCK cells were grown on 6 well plates for 24 h. The cells were washed and placed in serum-free MEM 17 h before infection. Stationary phase grown *P. aeruginosa* was added for 1 h. The infected monolayers were washed with cold PBS containing 1 mM sodium orthovanadate (Sigma-Aldrich). Cells were lysed in modified radioimmunoprecipitation assay (RIPA) buffer (50 mM Tris pH 7.4, 150 mM NaCl, 2 mM EDTA, 2 mM EGTA, 1% Triton X-100, 0.5% deoxycholate, 0.1% SDS, 1 mM sodium orthovanadate, 50 mM NaF, 1 mM phenylmethylsulfonyl fluoride (Sigma-Aldrich), and proteinase inhibitor cocktail (Sigma-Aldrich) for 20 min. The cell lysates were centrifuged at 16 000 *g* for 20 min. Protein concentration on the supernatant was determined by BCA method (Sigma-Aldrich) and typically 20 μg per line of total protein was electrophoresed on 8% SDS-polyacrylamide gels, and transferred to polyvinylidene difluoride membranes. The membranes were blocked with Tris Buffered Saline (TBS) containing 0.05% Tween 20 (TBST) and 5% non-fat milk or BSA for 1 h at room temperature and then incubated with the primary antibody. The membranes were washed with TBST, incubated with horseradish peroxidase-conjugated secondary antibody for 1 h at room temperature and developed using an enhanced chemiluminescence kit (Amersham Biosciences, Piscataway, NJ, USA).

RNA interference

Lyn constructs were made by annealing and ligating appropriate oligonucleotides (RNAi1 sense: CCGGGACCCTTCAACATGA CAAGCTCGAGCTTGTCATGTTGAAGGGTCTTTTTG; RNAi1 antisense: AATTCAAAAAGACCCTTCAACATGACAAGCTCGA GCTTGTCATGTTGAAGGGTC; RNAi2 sense: CCGGAGTGCT GCTTCCAAAGCTACTCGAGTAGCTTTGGAAGCAGCACTTTT TTG; RNAi2 antisense: AATTCAAAAAAGTGCTGCTTCCAAA GCTACTCGAGTAGCTTTGGAAGCAGCACT) into the AgeI and EcoRI cloning sites of pLKO.1-puro vector (details at http://www.addgene.org). These were sequenced and used to co-transfect human embryonic kidney 293 FT cells with Virapower lentiviral packaging mix (Invitrogen, Carlsbad, CA, USA). The next day, transfection complexes were removed and cells were allowed to produce virus for 24 h. Media containing virus were collected and used to directly transduce MDCK cells overnight. The cells were allowed to recover for 24 h and subject to puromycin selection (5 μg ml^{-1}). Silencing was confirmed by Western blot.

Statistical analysis

Data are shown as the mean ± standard deviation of at least three independent experiments. Student's *t*-test or nested ANOVA analysis were performed. *P*-value of < 0.05 was considered statistically significant.

Acknowledgements

We thank Joanne Engel, Anthony Pugsley, María Cecilia Larocca and Pablo S. Aguilar for critical reading of the manuscript. We thank Huga Naya for help with statistical analysis and Ariel Chaparro for technical support. This work was supported by Grant Number R03TW008056 from the Fogarty International Center, by Agencia Nacional de Investigación e Innovación (ANII) Program INNOVA URUGUAY-DCI- ALA/2007/19.040 URU-UE, FCE-2007 (A.K.), Sistema Nacional de Becas (P.L.) and by NIH grant 5P01 AI53194 (K.E.M.).

References

Allesen-Holm, M., Barken, K.B., Yang, L., Klausen, M., Webb, J.S., and Kjelleberg, S. *et al*. (2006) A characterization of DNA release in *Pseudomonas aeruginosa* cultures and biofilms. *Mol Microbiol* **59:** 1114–1128.

Bucior, I., Mostov, K., and Engel, J.N. (2010) *Pseudomonas aeruginosa*-mediated damage requires distinct receptors at the apical and basolateral surfaces of the polarized epithelium. *Infect Immun* **78:** 939–953.

Budrene, E.O., and Berg, H.C. (1991) Complex patterns formed by motile cells of *Escherichia coli*. *Nature* **349:** 630–633.

Budrene, E.O., and Berg, H.C. (1995) Dynamics of formation of symmetrical patterns by chemotactic bacteria. *Nature* **376:** 49–53.

Chung, J.W., Piao, Z.H., Yoon, S.R., Kim, M.S., Jeong, M., Lee, S.H., *et al*. (2009) *Pseudomonas aeruginosa* eliminates natural killer cells via phagocytosis-induced apoptosis. *PLoS Pathog* **5:** e1000561.

Clausen, C.R., and Christie, D.L. (1982) Chronic diarrhea in infants caused by adherent enteropathogenic *Escherichia coli*. *J Pediatr* **100:** 358–361.

Costerton, J.W., Stewart, P.S., and Greenberg, E.P. (1999) Bacterial biofilms: a common cause of persistent infections. *Science* **284:** 1318–1322.

Dacheux, D., Goure, J., Chabert, J., Usson, Y., and Attree, I. (2001) Pore-forming activity of type III system-secreted proteins leads to oncosis of *Pseudomonas aeruginosa*-infected macrophages. *Mol Microbiol* **40:** 76–85.

Darling, K.E., Dewar, A., and Evans, T.J. (2004) Role of the cystic fibrosis transmembrane conductance regulator in internalization of *Pseudomonas aeruginosa* by polarized respiratory epithelial cells. *Cell Microbiol* **6:** 521–533.

Dehio, C., Meyer, M., Berger, J., Schwarz, H., and Lanz, C. (1997) Interaction of *Bartonella henselae* with endothelial cells results in bacterial aggregation on the cell surface and the subsequent engulfment and internalisation of the bacterial aggregate by a unique structure, the invasome. *J Cell Sci* **110** (Pt 18)**:** 2141–2154.

Engel, J.N. (2003) Molecular pathogenesis of acute *Pseudomonas aeruginosa* infections. In *Severe Infections Caused by* Pseudomonas aeruginosa. Hauser, A., and Rello, J. (eds). New York: Kluwer Academic/Plenum Press, pp. 201–230.

Engen, J.R., Wales, T.E., Hochrein, J.M., Meyn, M.A., 3rd, Banu Ozkan, S., Bahar, I., and Smithgall, T. (2008) Structure and dynamic regulation of Src-family kinases. *Cell Mol Life Sci* **65:** 3058–3073.

Esen, M., Grassme, H., Riethmuller, J., Riehle, A., Fassbender, K., and Gulbins, E. (2001) Invasion of human epithelial cells by *Pseudomonas aeruginosa* involves src-like tyrosine kinases p60Src and p59Fyn. *Infect Immun* **69:** 281–287.

Evans, D.J., Frank, D.W., Finck-Barbançon, V., Wu, C., and Fleiszig, S.M. (1998) *Pseudomonas aeruginosa* invasion and cytotoxicity are independent events, both of which involve protein tyrosine kinase activity. *Infect Immun* **66:** 1453–1459.

Frick, I.M., Morgelin, M., and Bjorck, L. (2000) Virulent aggregates of *Streptococcus* pyogenes are generated by homophilic protein-protein interactions. *Mol Microbiol* **37:** 1232–1247.

Furumoto, Y., Gonzalez-Espinosa, C., Gomez, G., Kovarova, M., Odom, S., Parravicini, V., *et al*. (2004) Rethinking the role of Src family protein tyrosine kinases in the allergic response: new insights on the functional coupling of the high affinity IgE receptor. *Immunol Res* **30:** 241–253.

Guarino, M. (2010) Src signaling in cancer invasion. *J Cell Physiol* **223:** 14–26.

Hall-Stoodley, L., and Stoodley, P. (2009) Evolving concepts in biofilm infections. *Cell Microbiol* **11:** 1034–1043.

Hassett, D.J., Korfhagen, T.R., Irvin, R.T., Schurr, M.J., Sauer, K., Lau, G.W., *et al*. (2010) *Pseudomonas aeruginosa* biofilm infections in cystic fibrosis: insights into pathogenic processes and treatment strategies. *Expert Opin Ther Targets* **14:** 117–130.

Hawkins, P.T., Anderson, K.E., Davidson, K., and Stephens, L.R. (2006) Signalling through class I PI3Ks in mammalian cells. *Biochem Soc trans* **34:** 647–662.

Kannan, S., Audet, A., Knittel, J., Mullegama, S., Gao, G.F., and Wu, M. (2006) Src kinase Lyn is crucial for *Pseudomonas aeruginosa* internalization into lung cells. *Eur J immunol* **36:** 1739–1752.

Kannan, S., Audet, A., Huang, H., Chen, L.J., and Wu, M. (2008) Cholesterol-rich membrane rafts and Lyn are involved in phagocytosis during *Pseudomonas aeruginosa* infection. *J Immunol* **180:** 2396–2408.

Kazmierczak, B.I., Jou, T.-S., Mostov, K., and Engel, J. (2001) Rho-GTPase activity modulates *Pseudomonas aeruginosa* internalization by epithelial cells. *Cell Microbiol* **3:** 85–98.

Kierbel, A., Gassama-Diagne, A., Mostov, K., and Engel, J.N. (2005) The phosphoinositol-3-kinase-protein kinase B/Akt pathway is critical for *Pseudomonas aeruginosa* strain PAK internalization. *Mol Biol Cell* **16:** 2577–2585.

Kierbel, A., Gassama-Diagne, A., Rocha, C., Radoshevich, L., Olson, J., Mostov, K., and Engel, J. (2007) *Pseudomonas aeruginosa* exploits a PIP3-dependent pathway to transform apical into basolateral membrane. *J cell biol* **177:** 21–27.

Kreitzer, G., Schmoranzer, J., Low, S.H., Li, X., Gan, Y., Weimbs, T., *et al*. (2003) Three-dimensional analysis of post-Golgi carrier exocytosis in epithelial cells. *Nat Cell Biol* **5:** 126–136.

Lemon, K.P., Earl, A.M., Vlamakis, H.C., Aguilar, C., and Kolter, R. (2008) Biofilm development with an emphasis on *Bacillus subtilis*. *Curr Top Microbiol Immunol* **322:** 1–16.

Mairey, E., Genovesio, A., Donnadieu, E., Bernard, C., Jaubert, F., Pinard, E., *et al*. (2006) Cerebral microcirculation shear stress levels determine *Neisseria meningitidis* attachment sites along the blood-brain barrier. *J Exp Med* **203:** 1939–1950.

Menozzi, F.D., Boucher, P.E., Riveau, G., Gantiez, C., and Locht, C. (1994) Surface-associated filamentous hemagglutinin induces autoagglutination of *Bordetella pertussis*. *Infect Immun* **62:** 4261–4269.

Moreau-Marquis, S., Stanton, B.A., and O'Toole, G.A. (2008a) *Pseudomonas aeruginosa* biofilm formation in the cystic fibrosis airway. *Pulm Pharmacol Ther* **21:** 595–599.

Moreau-Marquis, S., Bomberger, J.M., Anderson, G.G., Swiatecka-Urban, A., Ye, S., O'Toole, G.A., and Stanton, B.A. (2008b) The DeltaF508-CFTR mutation results in increased biofilm formation by *Pseudomonas aeruginosa* by increasing iron availability. *Am J Physiol Lung Cell Mol Physiol* **295:** L25–L37.

Mougous, J.D., Gifford, C.A., Ramsdell, T.L., and Mekalanos, J.J. (2007) Threonine phosphorylation post-translationally regulates protein secretion in *Pseudomonas aeruginosa*. *Nat Cell Biol* **9:** 797–803.

Park, H.S., Wolfgang, M., van Putten, J.P., Dorward, D., Hayes, S.F., and Koomey, M. (2001) Structural alterations in a type IV pilus subunit protein result in concurrent defects in multicellular behaviour and adherence to host tissue. *Mol Microbiol* **42:** 293–307.

Pielage, J.F., Powell, K.R., Kalman, D., and Engel, J.N. (2008) RNAi screen reveals an Abl kinase-dependent host cell pathway involved in *Pseudomonas aeruginosa* internalization. *PLoS Pathog* **4:** e1000031.

Pier, G.B., Grout, M., Zaidi, T.S., Olsen, J.C., Johnson, L.G., Yankaskas, J.R., and Goldberg, J.B. (1996) Role of mutant CFTR in hypersusceptibility of cystic fibrosis patients to lung infections. *Science* **271:** 64–67.

Pier, G.B., Grout, M., and Zaidi, T.S. (1997) Cystic fibrosis transmembrane conductance regulator is an epithelial cell receptor for clearance of *Pseudomonas aeruginosa* from the lung. *Proc Nat Acad Sci USA* **94:** 12088–12093.

Schleheck, D., Barraud, N., Klebensberger, J., Webb, J.S., McDougald, D., Rice, S.A., and Kjelleberg, S. (2009)

Pseudomonas aeruginosa PAO1 preferentially grows as aggregates in liquid batch cultures and disperses upon starvation. *PLoS One* **4:** e5513.

Stoodley, P., Sauer, K., Davies, D.G., and Costerton, J.W. (2002) Biofilms as complex differentiated communities. *Annu Rev Microbiol* **56:** 187–209.

Susa, M., Rohner, D., and Bichsel, S. (1996) Differences in binding of PI 3-kinase to the src-homology domains 2 and 3 of p56 lck and p59 fyn tyrosine kinases. *Biochem Biophys Res Commun* **220:** 729–734.

Suzuki, T., Shoji, S., Yamamoto, K., Nada, S., Okada, M., Yamamoto, T., and Honda, Z. (1998) Essential roles of Lyn in fibronectin-mediated filamentous actin assembly and cell motility in mast cells. *J Immunol* **161:** 3694–3701.

Vanhaesebroeck, B., and Alessi, D.R. (2000) The PI3K-PDK1 connection: more than just a road to PKB. *Biochem J* **346** (Pt 3)**:** 561–576.

Yu, W., Datta, A., Leroy, P., O'Brien, L.E., Mak, G., Jou, T.S., *et al*. (2005) Beta1-integrin orients epithelial polarity via Rac1 and laminin. *Mol Biol Cell* **16:** 433–445.

Zhu, Q.S., Xia, L., Mills, G.B., Lowell, C.A., Touw, I.P., and Corey, S.J. (2006) G-CSF induced reactive oxygen species involves Lyn-PI3-kinase-Akt and contributes to myeloid cell growth. *Blood* **107:** 1847–1856.

Supporting information

Additional Supporting Information may be found in the online version of this article:

Fig. S1. SFKs are important for *P. aeruginosa* internalization into MDCK cells. Standard invasion and adhesion assays. MDCK cells were treated or not (control) with SU6656 (10 μM) or PP2 (10 μM). The number of internalized or attached bacteria for each well was normalized to the average number of internalized or attached bacteria for controls respectively. The normalized values were averaged to calculate the percentages of invasion and adhesion. Data are represented as mean ± standard deviation, *P < 0.05.

Fig. S2. Decreased expression of Lyn reduces internalization of *P. aeruginosa* into MDCK cells.

A. Standard invasion assays with MDCK cells expressing scramble (SC) or two different Lyn shRNAs (KD1 y KD2). The number of internalized bacteria for each well was normalized to the average number of adhered bacteria and to control (SC). The normalized values were averaged to calculate the percentages of invasion/adhesion.

B. Expression of Lyn in lysates of MDCK expressing SC or Lyn shRNAs was analysed by western blot. GAPDH was used as loading control; quantified in (C). Data are represented as mean ± standard deviation, *P < 0.05.

Video S1. Aggregates are formed on cell surface. Polarized MDCK grown on glass bottom dishes were infected with GFP *P. aeruginosa*. Images were collected every 3 s beginning immediately after inoculation of bacteria. Aggregates were formed from free-swimming bacteria that were recruited to localized spots on cell surface. Scale bar: 10 μm, time is shown in min : s.

Please note: Wiley-Blackwell are not responsible for the content or functionality of any supporting materials supplied by the authors. Any queries (other than missing material) should be directed to the corresponding author for the article.